ELSEVIER

Journal of Chromatography A, 818 (1998) 31–41

JOURNAL OF CHROMATOGRAPHY A

Immobilized metal affinity chromatography Self-sharpening of protein–modulator interfaces in frontal chromatography

Suresh Vunnum, Venkatesh Natarajan, Steven Cramer*

Department of Chemical Engineering, Rensselaer Polytechnic Institute, Troy, NY 12180, USA

Received 5 March 1998; received in revised form 4 May 1998; accepted 6 May 1998

Abstract

The binding behavior of mobile phase modulators in IMAC is quite different from that of proteins due to their single site interaction and high saturation capacities. Furthermore, stationary phase sites that are sterically shielded for proteins upon macromolecular adsorption are often accessible to mobile phase modifiers. In this paper, the implications of these differences on the self-sharpening of protein–modulator interfaces in frontal chromatography and on the order of elution in binary frontal chromatography are examined. A metal affinity interaction chromatography (MAIC) model is employed to study the behavior of these non-linear systems. The results indicate that for a given protein concentration, there exist a lower and an upper limit of modulator concentration that leads to a self-sharpening protein–modulator interface. Below the lower limit, a single step change in protein concentration can lead to the formation of two protein– modulator interfaces. In addition, protein–modulator binary frontal chromatography in IMAC systems is seen to exhibit dual selectivity reversals. The work presented in this paper has important implications for the determination of protein isotherms in IMAC systems.

Keywords: Mobile phase composition; Mobile phase modulators; Immobilized metal affinity chromatography; Self-sharpening protein–modulator interface; Frontal chromatography; Protein–modulator interface; Proteins

1. Introduction

Mobile phase modulators (MPMs) such as imidazole are widely used in chromatography to facilitate separations and to improve the time scales of operation. In most cases, they operate by interacting with the stationary phase, thereby competing with the proteins for the binding sites. However, the adsorption behavior of MPMs is often different from that of macromolecular solutes such as proteins. Proteins have multiple binding domains on their surface and hence exhibit multipoint interactions [1–3]. Furthermore, they sterically shield some of the stationary phase sites upon binding, rendering them inaccessible to other macromolecules [4,5]. In contrast, the MPMs typically used for separations have a single binding domain and are dramatically smaller than the proteins that are being separated. Thus, the sterically shielded sites that are inaccessible to macromolecules are often accessible to the MPMs.

In spite of these differences in the binding character between proteins and modulators, the Langmuirian isotherm has been employed to describe immobilized metal affinity chromatography (IMAC)

*Corresponding author.

0021-9673/98/$19.00
PII: S0021-9673(98)00411-7

systems [5,6]. The affinity constants determined using the Langmuir model are not adequate for predicting protein adsorption behavior as a function of modifier concentration. Furthermore, many of the assumptions implicit to the Langmuir isotherm are invalid for protein separations in IMAC systems. Previously, we have developed a metal affinity interaction chromatographic (MAIC) model [7] that is an extension of the generalized multi-component Langmuir formalism [8]. The MAIC model accounts for the multipoint attachment and steric shielding of the stationary phase sites upon protein binding. This model is therefore able to account for the differential saturation capacities as well as the modifier dependence of protein adsorption. This enables the prediction of a variety of complex experimental behaviors as observed in step gradient [7], linear gradient [9] and displacement operations [10]. The MAIC model has also been shown to accurately predict the concentration dependency of the displacer character of traditional MPMs in this system [10].

An understanding of the non-linear dynamics of protein chromatography in the presence of modulators is critical if one is to exploit the high selectivity obtainable in IMAC systems. In this manuscript the influence of modulator sorption on the self-sharpening of protein–modulator interfaces in frontal chromatography (FC) and the order of elution in binary frontal chromatography (BFC) is examined. FC is routinely employed for the measurement of isotherms [11,12]. Thus, for accurate determination of isotherm data, it is critical to know under what conditions the protein–modulator interface is self-sharpening.

2. Theory

2.1. Self-sharpening criteria

In this section, the self-sharpening criteria for the protein–modulator interface in frontal chromatography are presented. It is assumed that the protein–modulator interface reaches a coherent state and the velocities of the solutes on either side of this interface meet the coherence conditions [13,14].

2.1.1. Frontal chromatography

In this mode of chromatography, the column is initially equilibrated with the modulator and is subsequently loaded with a mixture of protein and modulator. The modulator concentration in the feed mixture and during equilibration are identical (see Fig. 1a). FC results in the formation of two distinct interfaces. These are denoted as interfaces I–II and II–III, respectively, in Fig. 1a. The protein–modulator interface II–III is self-sharpening only if the following inequalities hold simultaneously [8]:

$$\left(\frac{Q_p}{C_p}\right)_{C_{m,II},\ C_p\to 0} > \left(\frac{Q_p}{C_p}\right)_{C_{m,III},\ C_{p,III}} \quad (1)$$

$$\left(\frac{\partial Q_m}{\partial C_m}\right)_{C_{m,III},\ C_{p,III}} < \left(\frac{Q_p}{C_p}\right)_{C_{m,III},\ C_{p,III}} \quad (2)$$

where Q_p and C_p are the stationary and mobile phase concentrations of the protein, Q_m and C_m are the stationary and mobile phase concentrations of the modulator and the subscripts indicate the modulator and protein concentrations at which the quantities in parentheses are evaluated. For instance, the RHS in Eq. (1) means that the ratio (Q_p/C_p) is evaluated at the modulator and protein concentrations in zone III.

Eqs. (1) and (2) together test the self-sharpening

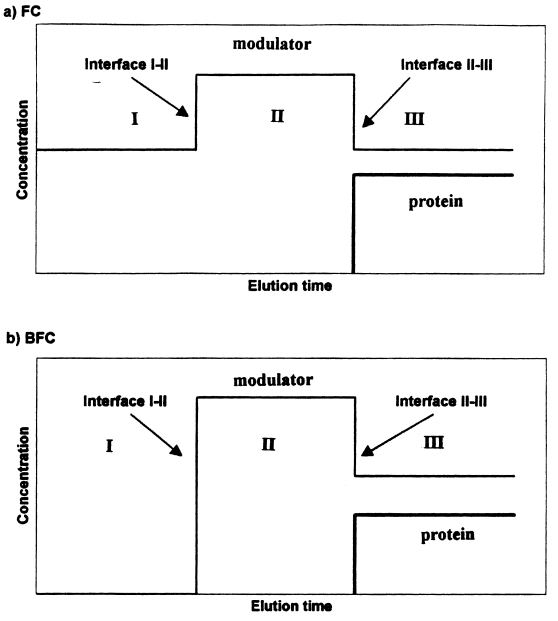

Fig. 1. Ideal breakthrough profiles. (a) FC; (b) BFC.

nature of the interface at the following points on the coherent boundary: ($C_{m,II}$, $C_p \rightarrow 0$) and ($C_{m,III}$, $C_{p,III}$). If Eqs. (1) and (2) are not satisfied, then the interface II–III is non-sharpening.

2.1.2. Binary frontal chromatography

In this mode, a binary mixture of protein and modulator is continuously introduced into a column in the absence of any prior equilibration with the modulator (see Fig. 1b). While Fig. 1b shows the order of elution as pure modulator followed by the protein–modulator interface, as will be shown below, the order of elution in BFC can also be pure protein followed by the protein–modulator interface. The order of elution is determined by the magnitude of the separation factor.

2.2. MAIC formalism

The MAIC model is a three-parameter model that incorporates mobile phase modifier effects and explicitly accounts for the multipointed nature of protein adsorption and the steric hindrance of the stationary phase sites upon binding of macromolecules. In this section we briefly review the model (for a detailed description refer to Ref. [7]).

Consider an iminodiacetic acid (IDA)–Cu(II) surface with a total capacity of Λ mM. Upon adsorption, the protein interacts with n_p sites on the stationary phase (number of interaction sites) and sterically hinders σ_p Cu^{2+} sites (steric factor). These sterically hindered sites are unavailable for the binding of other macromolecules in free solution. On the other hand, the sterically hindered sites are accessible to relatively small mobile phase modifiers such as imidazole. For a system of ''N'' proteins and a single mobile phase modifier, ''$N+1$'' equilibrium expressions can be written to represent multicomponent binding equilibria.

$$C_m + Q_v \Leftrightarrow Q_m \tag{3}$$

where subscript ''m'' refers to the mobile phase modifier with a single coordination site and Q_v refers to the sites available for the adsorption of the modifier on the stationary phase material.

$$C_p + n_p \bar{Q}_v \Leftrightarrow Q_p \quad p = 2,..., N+1 \tag{4}$$

where the subscript ''p'' refers to the proteins and $\bar{Q}_v$ represents vacant sites which are accessible for the adsorption of protein. The equilibrium constant K for this process is defined as

$$K_m = \frac{Q_m}{C_m Q_v} \tag{5}$$

for the modifier and as

$$K_p = \frac{Q_p}{C_p \bar{Q}_v^{n_p}} \tag{6}$$

for the protein.

Mass balance on the stationary phase yields

$$\Lambda = \bar{Q}_v + \bar{Q}_m + \sum_{p=2}^{N+1} (\sigma_p + n_p) Q_p \tag{7}$$

where $\bar{Q}_m$ refers to the modifier bound to the sterically unshielded copper sites on the stationary phase. Eqs. (5)–(7) together define protein multicomponent equilibria on IMAC surfaces in the presence of the modifier.

2.3. Mass transport equations

The model employed to describe mass transport in this work is the equilibrium-dispersive model [15]. Eq. (8) describes mass transport in the packed bed of a chromatographic column:

$$-D_i \frac{\partial^2 C_i}{\partial z^2} + u_0 \frac{\partial C_i}{\partial z} + \frac{\partial C_i}{\partial t} + \frac{1-\varepsilon}{\varepsilon} \frac{\partial Q_i}{\partial t} = 0 \tag{8}$$

where z is axial position, t is time, ε is the total porosity of the column, u_0 is related to the superficial velocity, u_s, by $u_0 = u_s/\varepsilon$, and D_i represents an effective dispersion coefficient. The stationary phase is assumed to be in equilibrium with the mobile phase:

$$Q_i = F_i(C_1, C_2,..., C_{N+1}) \tag{9}$$

The equilibrium expression F_i is the MAIC formalism discussed above. The above equations were solved in conjunction with the initial and boundary conditions corresponding to the two cases shown in Fig. 1:

Frontal chromatography:	Binary frontal chromatography:
I.C.	
$C_m(0,Z) = C_{m,f}$	$C_m(0,Z) = 0$
$C_p(0,Z) = 0$	$C_p(0,Z) = 0$
BC	
$C_m(t,0) = C_{m,f}$	$C_m(t > 0,0) = C_{m,f}$
$C_p(t > 0,0) = C_{p,f}$	$C_p(t > 0,0) = C_{p,f}$

(10)

2.4. Numerical method

In order to solve this system of partial differential equations, a finite difference numerical technique developed by Czok and Guiochon [15] was employed. In this technique, a simple relation exists between the observed efficiency of the chromatographic column, the effective dispersion coefficient of Eq. (8), and the dimensions of the finite difference grid:

$$\frac{H}{L} = \frac{2D_i}{Lu_0} = \Delta z - \frac{1}{1 + k'}\Delta\tau \quad (11)$$

where H is the height equivalent to a theoretical plate, L is the column length, k' is the capacity factor, Δz is the step size in the spatial dimension, and $\Delta\tau$ is the step size in the time dimension. Since the simulations were employed solely to study the effect of thermodynamics on the frontal profiles, a single dispersion coefficient has been employed for all the solutes. Based on the observed plate height for a typical protein, an effective dispersion coefficient of $2.0 \cdot 10^{-4}$ cm^2/s was employed in this study.

3. Experimental

3.1. Materials

Bulk chelating Superose (10 μm) containing covalently bound IDA donated by Pharmacia LKB Biotechnology (Uppsala, Sweden) was packed in a 57×5 mm I.D. glass column. A strong cation-exchange (SCX) (sulfopropyl, 8 μm, 50×5 mm I.D.) column was donated by Millipore (Waters Chromatography Division, Millipore, Milford, MA, USA). Bulk BioSeries SCX material (donated by Rockland Technologies, Newport, DE, USA) was packed in a 250×4.6 mm I.D. column. A POROS R/H reversed-phase chromatographic column (100×4.6 mm I.D.) was obtained from PerSeptive Biosystems (Cambridge, MA, USA). Acetonitrile was purchased from Fisher Scientific (Fairlawn, NJ, USA). Sodium chloride, sodium monobasic phosphate, sodium dibasic phosphate, sodium acetate, cupric sulfate, ethylenediamine tetraacetic acid (EDTA), imidazole and all proteins were purchased from Sigma (St. Louis, MO, USA).

3.2. Apparatus

The system consisted of two Model P-500 pumps (Pharmacia) connected to the chromatographic column via a Model MV-7 injector (Pharmacia). Fractions of the column effluent were collected from the frontal chromatography experiments using a Model 2212 Helirac fraction collector (Pharmacia). The collected fractions were subsequently analyzed for protein and modulator concentrations. A Spectroflow 757 UV–Vis absorbance detector (Applied Biosystems, Foster City, CA, USA) was employed to monitor the column effluent, and a Model C-R3A Chromatopac integrator (Shimadzu, Kyoto, Japan) was employed for data acquisition and analysis.

3.3. Procedures

3.3.1. Immobilization of Cu^{2+}

The IDA column was washed with 10 column volumes of distilled water and subsequently loaded with copper ions by equilibration with an aqueous solution of 0.3 *M* copper sulfate, pH 3.9. Unadsorbed metal ions were removed by washing the IDA–Cu(II) column with five column volumes of 0.1 *M* sodium acetate, pH 4.0. The column was then washed with three column volumes of distilled water and equilibrated with the appropriate buffer solution.

3.3.2. FC of proteins

The carrier buffer employed in all experiments contained 0.5 *M* NaCl in 50 m*M* phosphate buffer, pH 7.0. Imidazole was employed as the mobile phase modulator in this study. All the experiments were carried out at room temperature at a flow-rate of 0.2 ml/min. Fractions were collected directly from the column effluent and analyzed as described below. Details of the individual experiments are given in the figure legends.

3.3.3. Determination of MAIC parameters

The linear adsorption parameters of the proteins, the number of interaction sites (n_p), and the equilibrium constant (K_p), were estimated from linear elution experiments at various carrier MPM concentrations. The steric factors (σ_p) were obtained from nonlinear frontal experiments carried out over a range of MPM concentrations. Imidazole MAIC parameters were obtained by fitting the isotherm data points to the single component Langmuir isotherm. For a detailed discussion of these parameter estimation techniques, the reader is referred to Ref. [7].

3.3.4. Regeneration

In order to ensure that the total bed capacity remained constant, after each experiment, the column was washed with 10 column volumes of deionized water, stripped of Cu^{2+} ions by washing with five column volumes of 0.1 *M* EDTA, and washed with a further 10 column volumes of deionized water. The immobilization of Cu^{2+} was then carried out as described in Section 3.3.1.

3.3.5. Effluent analysis by high-performance liquid chromatography (HPLC)

Effluent fractions obtained from the frontal chromatography experiments were diluted 5–100-fold, and 25-μl samples were analyzed using the following methods. The effluent was monitored at 280 nm for the proteins and at 400 nm for imidazole.

3.3.5.1. Imidazole analysis

Isocratic chromatography was performed on a 250×4.6 mm I.D. SCX column using a carrier of 15 m*M* phosphate buffer, pH 5.0, and a flow-rate of 0.9 ml/min.

3.3.5.2. Ribonuclease A (RNAse A) analysis

Isocratic chromatography was performed on a 50×5 mm I.D. SCX column using a carrier of 50 m*M* phosphate buffer, pH 6.0, containing 60 m*M* NaCl and a flow-rate of 0.5 ml/min.

3.3.5.3. Myoglobin analysis

Isocratic chromatography was performed on a 100×4.6 mm I.D. POROS reversed-phase column using a carrier of 38% (v/v) acetonitrile in 50 m*M* phosphate buffer, pH 2.2, at a flow-rate of 0.9 ml/min.

4. Results and discussion

The model parameters for the proteins employed in this study and the imidazole modifier were determined as described in Section 3 and are presented in Table 1.

When the Eqs. (1) and (2) are satisfied, interface II–III in Fig. 1a is self-sharpening. A simulation result of such a scenario for the imidazole–RNAse A system in IMAC is presented in Fig. 2. As expected, the positive imidazole system peak travels ahead of the protein–imidazole interface.

At a given protein concentration, there exists a lower and an upper limit of modulator concentration within which Eqs. (1) and (2) are satisfied. Outside this range, the interface in non-sharpening. The

Table 1
MAIC adsorption parameters of the solutes employed in this study

Solute	Interaction sites, n_i	Equilibrium constant, K_i (mM^{-n_i})	Steric factor, σ_i
Ribonuclease A (bovine pancreas)	1.81	$2.1 \cdot 10^{-1}$	4.1
Myoglobin (horse heart)	3.3	$6.6 \cdot 10^{-2}$	3.0
Conalbumin (hen egg)	4.7	$3.0 \cdot 10^{-5}$	18.0
Imidazole	1.0	3.55	0.0

Phase ratio: 0.24.
Bed capacity (Λ): 201.5 m*M*.

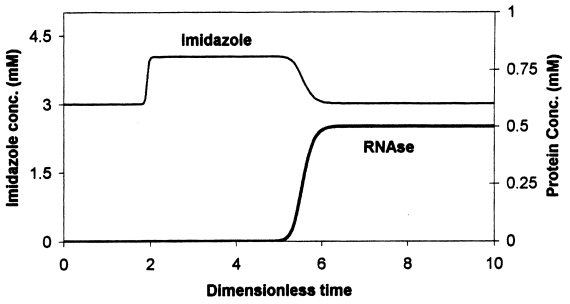

Fig. 2. Simulation result of a self-sharpening imidazole–RNAse A interface. Equilibration imidazole concentration 3 m*M*; feed consisted of 0.5 m*M* RNAse A in 3 m*M* imidazole.

modulator dependency of the three terms involved in Eqs. (1) and (2) at a fixed protein concentration are depicted in Fig. 3a (note: see Appendix A for calculations). For modulator concentrations in the region indicated in the figure, interface II–III (Fig. 1a) is self-sharpening.

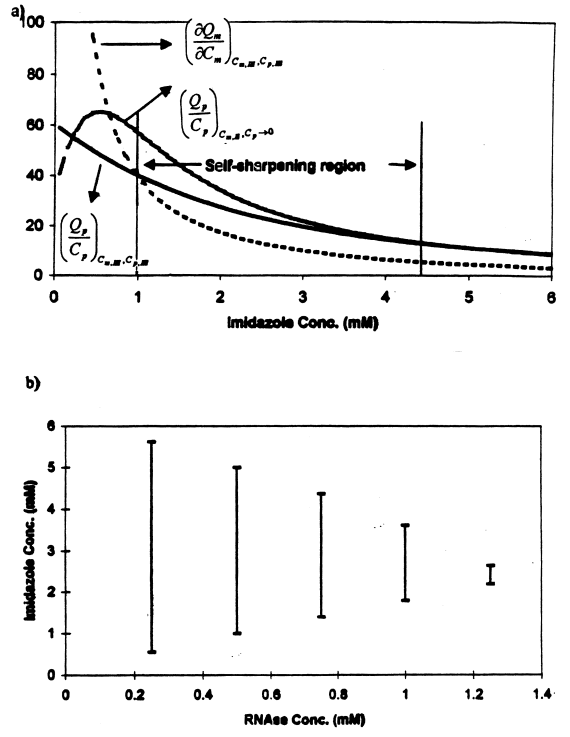

Fig. 3. (a) Modulator concentration dependency of the three terms in Eqs. (1) and (2). The protein employed was RNAse A and its concentration was fixed at 0.5 m*M*. (b) Variation of the upper and lower limits of imidazole concentrations over which interface II–III (Fig. 1a) is self-sharpening, as a function of the RNAse A concentration.

A non-sharpening protein–modulator interface is normally expected under high modulator concentrations where the protein adsorption is relatively weak. However, in IMAC, the difference in the modulator concentrations across interface II–III (Fig. 1a) is higher at lower modulator concentrations. In addition, the ability of the modulator to bind to sites which are unavailable for the protein (i.e., sterically shielded) results in a lowered attenuation of its binding in the presence of the protein. Thus, for a given protein concentration, there exists a lower limit of the modulator concentration for interface II–III (Fig. 1a) to be self-sharpening.

The lower and upper limit of the modulator concentration, for which interface II–III (Fig. 1a) is self-sharpening, is a function of the protein concentration. The variation of these limits of imidazole concentration as a function of RNAse A concentration is shown in Fig. 3b. As seen in the figure, as the protein concentration increases, the modulator concentration range for self-sharpening decreases. Beyond an RNAse A concentration of 1.25 m*M*, there exists no modulator concentration for which interface II–III is self-sharpening.

The simulation result and the experimental verification of conditions yielding a non-sharpening interface is shown in Fig. 4. The simulation and experiment correspond to a case where the column is initially equilibrated with 0.8 m*M* imidazole, and subsequently loaded with 1.25 m*M* RNAse A in 0.8 m*M* imidazole. In this case, the modulator concentration is below the lower limit of the range in which the interface is self-sharpening. As seen in the figure, the nature of the breakthrough profile of RNAse A is well predicted by the model. The plateau concentration of the imidazole system peak and the breakthrough volume of RNAse A are both in good agreement with the simulation. Furthermore, the outlet concentration of the protein attains the feed value asymptotically in both experiment and simulation.

Fig. 5 shows the simulation result and the experimental verification of the condition yielding two coherent protein–modulator interfaces. The column was initially equilibrated with 4 m*M* of imida-

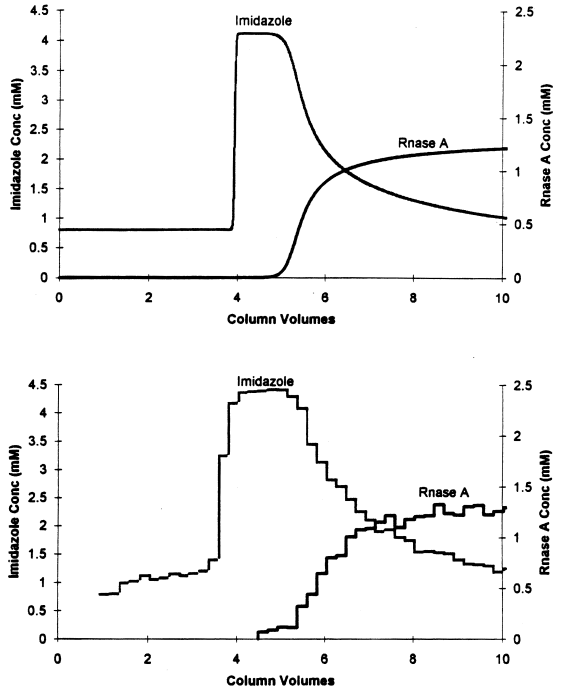

Fig. 4. Comparison of simulated and experimental breakthrough profiles under conditions where the modulator concentration is below the lower limit defining self-sharpening behavior. (a) Simulation result; (b) experimental profile. The column was initially equilibrated with a solution of 0.8 m*M* imidazole in buffer (0.5 *M* NaCl, 50 m*M* phosphate, pH 7) and subsequently loaded with a front of 1.25 m*M* RNAse A in the buffer solution containing 0.8 m*M* imidazole.

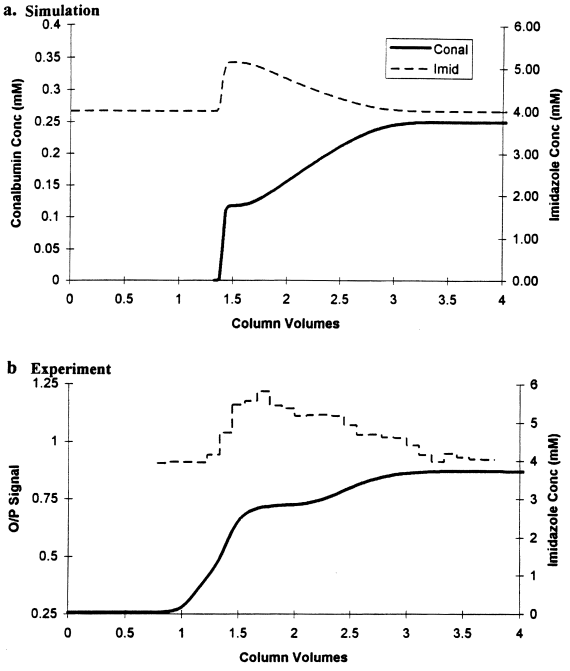

Fig. 5. Comparison of simulated and experimental chromatograms under conditions leading to two protein–modulator interfaces. (a) Simulation result; (b) experimental profile. The column was initially equilibrated with a solution of 4 m*M* imidazole in buffer (0.5 *M* NaCl, 50 m*M* phosphate, pH 7) and subsequently loaded with a front of 0.25 m*M* conalbumin in the buffer solution with 4 m*M* imidazole.

zole, and subsequently loaded with 0.25 m*M* conalbumin in 4 m*M* imidazole. As predicted by the model, a single step change in the protein concentration at the column inlet leads to two distinct protein–modulator interfaces separated by a plateau region. In such systems, the earlier eluting protein–modulator interface is necessarily self-sharpening as the concentrations of both the protein and the modulator increase across it. On the other hand, the later eluting interface may or may not be self-sharpening.

These results demonstrate that at modulator concentrations below the lower limit, frontal chromatography can result in either a single, non-sharpening protein–modulator interface or two coherent protein–modulator interfaces. It turns out that, at modulator concentrations above the upper limit, a single, non-sharpening protein–modulator interface is always obtained.

4.1. Order of elution in BFC

The order of elution in BFC (Fig. 1b) is governed by the magnitude of the separation factor. In the MAIC formalism, the separation factor is a function of both the protein and modulator concentrations (Appendix B). For the elution order in BFC to be pure modulator followed by a mixed zone of protein and modulator:

$$\alpha_{mp} < 1 \tag{12}$$

where α_{mp} is the separation factor of the modulator–protein pair.

The variation of the separation factor as a function of both imidazole and myoglobin concentrations is

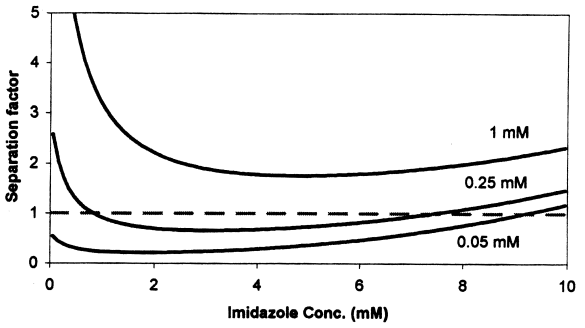

Fig. 6. The variation of protein–modulator separation factor as a function of protein and modulator concentrations. Protein: myoglobin. Modulator: imidazole.

shown in Fig. 6. In this plot, the region above $\alpha_{mp}=1$ corresponds to the elution order of pure myoglobin followed by a mixed zone of myoglobin and imidazole. As seen in this figure, at a myoglobin concentration of 0.25 m*M*, the curve intersects the $\alpha_{mp}=1$ line twice at imidazole concentrations of 0.8 and 7.5 m*M*. At very low imidazole concentration (<0.8 m*M*) the elution order is pure protein followed by a mixed zone of protein and imidazole. This is not due to the higher affinity of the modulators but is rather due to their high saturation capacity and their ability to bind to stationary phase sites that are sterically shielded for proteins upon macromolecular adsorption. Increasing the imidazole concentrations beyond 0.8 m*M* leads to a selectivity reversal and an elution order of pure imidazole followed by a mixed zone of myoglobin and imidazole. Further increasing the imidazole concentration beyond 7.5 m*M* reverts the selectivity and restores the original order. Under these conditions, the selectivity reversal is due primarily to the affinity and mass action of the modulators (i.e., the displacement effect). Thus, under these conditions, the order of elution in BFC exhibits dual selectivity reversals.

In contrast, when the myoglobin concentration is increased to 1 m*M*, the plot of separation factor (Fig. 6) lies entirely in the region above $\alpha_{mp}=1$ and thus does not exhibit any selectivity reversal. Finally, for a lower myoglobin concentration (0.05 m*M*) the system exhibits only a single transition corresponding to the displacement effect.

4.2. Simulations and experimental verification of selectivity reversals in BFC

Figs. 7 and 8 show the simulation results and the experimental verifications of selectivity reversals for the myoglobin–imidazole IMAC system. In these experiments, the imidazole concentration was fixed at 6 m*M*, and the myoglobin concentrations were varied. At a myoglobin concentration of 0.2 m*M*, the elution order was pure imidazole followed by a mixed zone of myoglobin and imidazole (Fig. 7). On the other hand, when the myoglobin concentration was increased to 0.7 m*M*, the elution order was pure myoglobin followed by a mixed zone of myoglobin and imidazole (Fig. 8). While the experimental results under these conditions corroborated the reversal in elution order, the high concentrations of

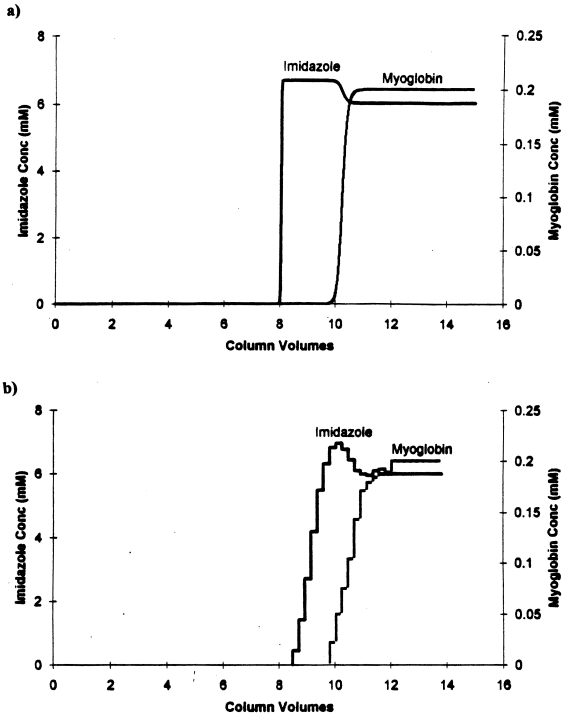

Fig. 7. Comparison of simulated and experimental profiles in binary frontal chromatography. A binary front of 0.2 m*M* myoglobin and 6 m*M* imidazole in buffer (0.5 *M* NaCl, 50 m*M* phosphate, pH 7.0) was loaded onto the column. (a) Simulated profile; (b) experimental result.

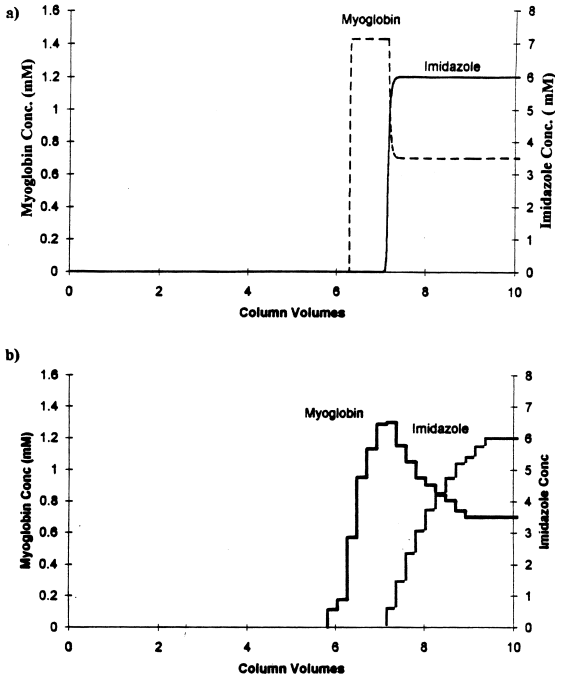

Fig. 8. Comparison of simulated and experimental profiles in binary frontal chromatography. A binary front of 0.7 m*M* myoglobin and 6 m*M* imidazole in buffer (0.5 *M* NaCl, 50 m*M* phosphate, pH 7.0) was loaded onto the column. (a) Simulated profile; (b) experimental result.

myoglobin produced in Fig. 8 resulted in some viscous fingering, which produced a more dispersed experimental profile.

5. Implications

5.1. Isotherm measurement in the presence of modulators

Modulators are widely used in chromatography to facilitate separations. The optimization and scale-up of separations therefore requires an accurate quantification of protein binding in the presence of modulators. FC is widely employed for this purpose [11,12]. The results of the current study indicate that the practice of employing FC for isotherm measurements in the presence of modulators may not be valid under all operating conditions in IMAC. The protein– modulator interface is not always self-sharpening. When the modulator concentration is below the lower limit for the protein–modulator interface to be self-sharpening (Fig. 3a), the outlet protein concentration attains the feed value asymptotically (Fig. 4). In this case, the use of the inflection point would give erroneous results. Further, if integration of the protein breakthrough profile is employed to determine the isotherm, the column has to be loaded with the feed solution for inordinately long times in order to obtain accurate values. On the other hand, under conditions where a single step change in protein concentration leads to the formation of two protein–modulator interfaces (Fig. 5), FC cannot be employed for the quantification of the protein adsorption isotherm.

The simulations presented in Fig. 4a and Fig. 5a were carried out under essentially equilibrium adsorption conditions with minimal mass transport effects. Nevertheless, under these conditions, the breakthrough profiles of the protein exhibited behavior usually attributed to transport and/or kinetic effects [16,17]. These results are quite important in that they indicate that an examination of the protein breakthrough profiles alone may lead one to erroneously conclude that the mass transfer characteristics of the column were poor. The results presented in this paper demonstrate the importance of accurately describing mobile phase modifier effects in non-linear IMAC FC systems.

6. Nomenclature

C	Mobile phase concentration of species (m*M*)
D	Axial dispersion coefficient (cm^2/s)
K	Equilibrium constant (mM^{-n})
n	Number of interaction sites on solute
$\bar{Q}_v$	Concentration of stationary phase sites accessible for adsorption of proteins (m*M*)
Q	Stationary phase concentration of species (m*M*)
u_0	Chromatographic velocity (cm/s)
u_s	Superficial velocity (cm/s)
t	Time (s)

t_o Time taken by an unretained tracer to traverse the column (s)
z Axial distance (cm)

6.1. Greek

α Separation factor
σ Steric factor of solute
Λ Bed capacity of column (mM)
ε Total porosity of column
τ Dimensionless time ($=t/t_o$)

6.2. Subscripts

m Modulator
p Protein
f Feed

Acknowledgements

This research was supported by Pharmacia Biotech (Uppsala, Sweden) and Grant No. CTS-9416921 from the National Science Foundation.

Appendix A

Magnitude of imidazole system peak

Equating the velocities of the protein and modulator fronts in interface II–III (Fig. 1a), we get the following quadratic equation for $C_{m,II}$:

$$K_m C_{m,II}^2 + \left(1 - K_m C_{m,III} - \frac{\Lambda K_m}{K_p \bar{Q}_v^{n_p}} + \frac{Q_{m,III}}{K_p \bar{Q}_v^{n_p}}\right) C_{m,II} + \left(\frac{Q_{m,III}}{K_p \bar{Q}_v^{n_p}} - C_{m,III}\right) = 0 \quad \text{(A1)}$$

$$Q_{m,III} = \frac{\Lambda K_m C_{m,III}}{1 + K_m C_{m,III}} \quad \text{(A2)}$$

$$\Lambda = \bar{Q}_v + K_m C_{m,III} \bar{Q}_v + (n_p + \sigma_p) K_p C_{p,III} \bar{Q}_v^{n_p} \quad \text{(A3)}$$

Eq. (A2) is the single component isotherm for imidazole and Eq. (A3) is a stationary phase site balance. A Newton–Raphson technique was employed to solve for $\bar{Q}_v$ using A3. Then, using Eqs. (A1) and (A2), the magnitude of the imidazole system peak, $C_{m,II}$, was computed.

Inequalities 1 and 2 (Eqs. (1) and (2))

Knowing $C_{m,II}$, $Q_{m,II}$ and $\bar{Q}_v$, the various terms in Eqs. (1) and (2) were computed as follows:

$$\left(\frac{Q_p}{C_p}\right)_{C_{p\to 0}}^{C_{m,II}} = \frac{K_p \Lambda^{n_p}}{(1 + K_m C_{m,II})^{n_p}} \quad \text{(A4)}$$

$$\left(\frac{Q_p}{C_p}\right)_{C_{p,III}}^{C_{m,III}} = K_p \bar{Q}_v^{n_p} \quad \text{(A5)}$$

$$\left(\frac{\partial Q_m}{\partial C_m}\right)_{C_{p,III}}^{C_{m,III}} = K_m \bar{Q}_v + K_m C_m \frac{\partial \bar{Q}_v}{\partial C_m} + \frac{\sigma_p Q_{p,III} K_m + \sigma_p K_m C_m \dfrac{\partial Q_{p,III}}{\partial C_m}}{(1 + K_m C_m)^2} \quad \text{(A6)}$$

In order to solve Eq. (A6), the two derivative terms must be computed.

$$Q_{p,III} = K_p C_{p,III} \bar{Q}_v^{n_p} \quad \text{(A7)}$$

Thus, for a given protein concentration,

$$\frac{\partial Q_{p,III}}{\partial C_{m,III}} = K_p C_{p,III} n_p \bar{Q}_v^{n_p - 1} \frac{\partial \bar{Q}_v}{\partial C_{m,III}} \quad \text{(A8)}$$

Differentiating Eq. (A3) with $C_{m,III}$ for a given protein concentration yields

$$\frac{\partial \bar{Q}_v}{\partial C_{m,III}} = \frac{K_m \bar{Q}_v}{1 + K_m C_{m,III} + (\sigma_p + n_p) K_p C_{p,III} n_p \bar{Q}_v^{n_p - 1}} \quad \text{(A9)}$$

Thus, using Eqs. (A7)–(A9), the LHS of Eq. (A6) can be computed.

Fig. 3 plots $\left(\frac{Q_p}{C_p}\right)_{C_{m,II}, C_{p\to 0}}$, $\left(\frac{Q_p}{C_p}\right)_{C_{m,III}, C_{p,III}}$ and $\left(\frac{\partial Q_m}{\partial C_m}\right)_{C_{m,III}, C_{p,III}}$ versus $C_{m,III}$ for a fixed protein concentration, $C_{p,III}$.

Appendix B

Dependence of separation factor on modulator concentration

By definition,

$$\alpha_{mp} = \frac{Q_m / C_m}{Q_p / C_p} \tag{B1}$$

From the MAIC model,

$$Q_m = \frac{(\Lambda - n_p Q_p) K_m C_m}{1 + K_m C_m} \tag{B2}$$

Combining Eqs. (B2) and (A7), one obtains the following

$$\alpha_{mp} = \frac{\left(\Lambda - n_p K_p C_p \bar{Q}_v^{n_p}\right) K_m}{(1 + K_m C_m) K_p \bar{Q}_v^{n_p}} \tag{B3}$$

Eq. (B3) describes the dependence of the separation factor on the modulator concentration for a given protein concentration. Fig. 6 was generated as follows: for a given protein concentration, $\bar{Q}_v$ was computed for various modulator concentrations by solving Eq. (A3) using a Newton–Raphson technique. These values of $\bar{Q}_v$ were subsequently substituted in Eq. (B3) to generate the plots shown in Fig. 6.

References

[1] W. Kopaciewicz, M.A. Rounds, J. Fausnaugh, F.E. Regnier, J. Chromatogr. 266 (1983) 3–21.
[2] M.A. Rounds, F.E. Regnier, J. Chromatogr. 283 (1984) 37.
[3] R.J. Todd, R.D. Johnson, F.H. Arnold, J. Chromatogr. A 662 (1994) 13–26.
[4] C.A. Brooks, S.M. Cramer, AIChE J. 38 (1992) 1969–1978.
[5] M. Belew, T.T. Yip, L. Andersson, J. Porath, J. Chromatogr. 403 (1987) 197.
[6] T.W. Hutchens, T.T. Yip, Anal. Biochem. 191 (1990) 160–168.
[7] S. Vunnum, S.R. Gallant, Y. Kim, S.M. Cramer, Chem. Eng. Sci. 11 (1995) 1785–1803.
[8] F.D. Antia, Cs. Horvath, J. Chromatogr. 556 (1991) 119–143.
[9] S. Vunnum, V. Natarajan, S.R. Gallant, S.M. Cramer, Sep. Sci. Tech., submitted for publication.
[10] S. Vunnum, S.R. Gallant, S.M. Cramer, Biotech. Prog. 12 (1996) 84–91.
[11] J. Jacobson, J. Frenz, Cs. Horvath, Ind. Eng. Chem. Res. 26 (1987) 43.
[12] J. Jacobson, J. Frenz, J. Chromatogr. 499 (1990) 5.
[13] G.F. Helfferich, G. Klein, Multicomponent Chromatography, Marcel Dekker, New York, 1970.
[14] G.F. Helfferich, R.D. Whitley, J. Chromatogr. A 734 (1996) 7.
[15] M. Czok, G. Guiochon, Anal. Chem. 62 (1990) 189–200.
[16] R.D. Whitley, K.E. Van Cott, N.H.L. Wang, Ind. Eng. Chem. Res. 32 (1993) 149–159.
[17] G.F. Helfferich, P.W. Carr, J. Chromatogr. 629 (1993) 97.